Journal of Ovarian Research

RESEARCH

Open Access

Tumour-derived exosomal miR-205 promotes ovarian cancer cell progression through M2 macrophage polarization via the PI3K/Akt/mTOR pathway

Liuqing He[1,2], Quan Chen[2] and Xiaoying Wu[2,3*]

Abstract

Background Tumour-associated macrophages (TAMs) are the most abundant immune cells in the tumour environment and are considered similar to M2 macrophages, which facilitate cancer progression. Exosomes, as important mediators of the cross-talk between tumour cells and tumour-associated macrophages, can facilitate the development and metastasis of ovarian cancer by mediating M2 macrophage polarization. However, the exact mechanisms underlying the communication between ovarian cancer (OC) cells and tumour-associated macrophages during OC progression remain unclear.

Results Here, we demonstrated that high expression of miR-205 was associated with M2 macrophage infiltration, which affected the prognosis of OC patients. Importantly, tumour-derived miR-205 could be transported from OC cells to macrophages via exosomes and promote cancer cell invasion and metastasis by inducing M2-like macrophage polarization. Animal experiments further confirmed that exosomal miR-205-induced M2 macrophages accelerated OC progression in vivo. Mechanistically, miR-205 downregulated PTEN, activating the PI3K/AKT/mTOR signalling pathway, which is critical for M2 polarization.

Conclusions These results reveal that exosomal miR-205 plays a pivotal role in macrophage polarization within the OC microenvironment, highlighting its potential as a therapeutic target for OC treatment. This study not only enhances our understanding of the interactions between tumour and immune cells but also opens new avenues for targeted therapies against exosomal miR-205 in ovarian cancer.

Keywords Exosomes, miR-205, Ovarian cancer, Macrophage polarization, PI3K/AKT/mTOR pathway

*Correspondence:
Xiaoying Wu
xyw2007@csu.edu.cn
[1]Department of Pathology, The Second Xiangya Hospital, Central South University, Changsha, Hunan 410011, China
[2]Department of Pathology, School of Basic Medical Science, Central South University, Changsha, Hunan 410013, China
[3]Department of Pathology, Xiangya Hospital, Central South University, Changsha, Hunan 410078, China

Background

Ovarian cancer (OC) is the most lethal malignant gynaecological tumour of the reproductive system [1, 2] and is characterized by complex interactions within its tumour microenvironment (TME) [3–6]. A key player in the TME is tumour-associated macrophages (TAMs), which can polarize into two distinct phenotypes: M1 and M2 [7, 8]. M1 macrophages are known for their proinflammatory properties and are linked to antitumour responses, whereas M2 macrophages tend to have immunosuppressive functions and are thought to aid in tumour progression and metastasis [9, 10]. The polarization of TAMs is influenced by various factors, including cytokines and microRNAs (miRNAs), which play significant roles in regulating gene expression and cellular processes within the TME [11–13].

Recent research has increasingly focused on how cell–cell communication can occur through exosomes, which are small extracellular vesicles released by different cell types [14–16]. Exosomes are extracellular vesicles released from various cell types and contain numerous molecules from the parental cells, including miRNAs, proteins and nucleic acids [17, 18]. The transfer of miRNAs by exosomes is especially interesting since exosomal miRNAs released from cancer cells can stimulate macrophages to switch their phenotype and play a role in promoting cancer progression and metastasis [19, 20]. Recent studies have highlighted the pivotal role of miR-205 in cancer biology, particularly in the context of OC. miR-205 is implicated in the regulation of multiple cellular functions, including the proliferation, apoptosis, and migration of cancer cells [21, 22]. Here, we showed that miR-205 could modulate TAM polarization, promoting the M2 phenotype and thereby enhancing the tumour-promoting effects of macrophages. This interaction underscores the potential of miR-205 as a target for therapeutic interventions aimed at reprogramming the immune landscape in ovarian cancer.

The intricate relationship between TAMs and miRNAs in OC represents a promising area of investigation. Despite the accumulating evidence regarding their roles, several molecular mechanisms underlying TAM polarization and the specific contributions of miR-205 remain inadequately understood [23]. Recent studies have highlighted how TAMs can be educated by tumour-derived signals, particularly in hypoxic environments, leading to a shift in their functional phenotypes towards a protumourigenic state. For example, Chen et al. reported that exosomes derived from hypoxic epithelial ovarian cancer (EOC) cells can induce the M2 polarization of macrophages, thereby promoting tumour proliferation and migration through a feedback loop involving specific miRNAs enriched in these exosomes, such as miR-222-3p and miR-223 [24]. Furthermore, Zhou et al. identified that exosomal miRNAs from TAMs can modulate Treg/Th17 cell ratios, contributing to an immunosuppressive microenvironment that favours EOC progression [25]. These findings suggest that miRNAs play a critical role in mediating the communication between TAMs and cancer cells, potentially serving as therapeutic targets or biomarkers. Moreover, the involvement of specific miRNAs, such as miR-205, in the polarization process remains to be fully elucidated. While miR-205 has been implicated in various cancer-related pathways, its exact role in TAM modulation and the resulting effects on tumour behaviour in OC are still under investigation. Understanding how miR-205 and other miRNAs influence TAM behaviour could lead to the development of novel therapeutic strategies aimed at reprogramming the TME to inhibit OC progression.

This study addresses these gaps in knowledge by adopting a comprehensive approach that includes the use of human tissue samples, in vitro cell culture, and advanced molecular techniques such as RNA interference and exosome characterization. The goal of this study is to clarify how tumour-derived exosomal miR-205 affects TAM polarization and the subsequent behaviours of tumour cells, including proliferation and invasion, within the OC microenvironment. A deeper understanding of the interaction between miR-205 and TAMs could reveal new therapeutic targets and strategies aimed at reprogramming the immune response in ovarian cancer patients.

In conclusion, exploring the relationship between miR-205 and TAM polarization offers a promising path for enhancing our understanding of OC biology and improving therapeutic outcomes. By examining the specific roles of tumour-derived exosomal miR-205 in shaping the immune landscape, this research contributes to the development of targeted therapies that could increase the effectiveness of current treatment options and ultimately improve the prognosis of patients with ovarian cancer.

Methods

Human tissue collection

A total of 74 cases of formalin-fixed paraffin-embedded samples, including 34 OC tissue specimens, 20 normal ovarian tissue specimens and 20 metastatic tissues, were collected from OC patients who underwent curative-intent surgery without prior radiotherapy and chemotherapy between 2014 and 2018 at the Department of Pathology, Xiangya Hospital of Central South University (CSU). All specimen diagnoses were confirmed by a qualified pathologist after surgery. The study was approved by the Institutional Ethics Committee of Xiangya Hospital of CSU and was conducted following the ethical guidelines of the Declaration of Helsinki. Each participant signed an informed consent form.

Cell culture

The epithelial OC cell lines HO-8910 and the monocytic cell line THP-1 were obtained from the Chinese Academy of Sciences Cell Bank and had been purchased from China Center for Type Culture Collection (CCTCC) and Cell Resource Center, IBMS, CAMS/PUMC (CRC/PUMC). HO-8910 cells stably overexpressing miR-205 and negative control cells were established by the Xiaoying Wu research group of the pathology laboratory of CSU, and the transfection efficiency was verified in a previous study [21]. All cell lines were cultured in DMEM or RPMI 1640 medium (Thermo Scientific, Waltham, MA, USA) supplemented with 10% foetal bovine serum (FBS) (Gibco, Gaithersburg, MD, USA). THP-1 cells (1×10^6) were incubated with 100 ng/ml phorbol 12-myristate 13-acetate (PMA) (Solarbio, Beijing, China) for 24–48 h in vitro to induce their differentiation into macrophages. For the exosome treatment experiments, 1 μg/ml exosomes was added to the culture medium of recipient cells (2×10^5).

Immunohistochemistry (IHC) and in situ hybridization (ISH)

A total of 74 paraffin-embedded OC tissues were assessed by IHC and ISH staining. The macrophage marker CD68 and the M2-type macrophage marker CD163 expression were measured with anti-CD68 (1:200, Abcam, Cambridge, UK) and anti-CD163 (1:200, Abcam) antibodies. ISH was performed on OC tissue samples using an LNA microRNA ISH miR-205 optimization kit (Exiqon; Woburn, MA, USA). The stained slides were scanned and photographed using digital pathological scanning equipment. The final score obtained from the Image-Pro plus (IPP, version 5.0, Media Cybernetics, Silver Spring, MD) analysis was used to identify the relative level of CD68, CD163 and miR-205 expression according to a previous study [22]. The positivity rate was calculated as the integral optical density (IOD)/area sum. ISH was conducted on OC tissue specimens utilizing an LNA™ microRNA ISH miR-205 optimization kit (Exiqon; Woburn, MA, USA). Following the manufacturer's instructions, paraffin-embedded tissue specimens were sliced into 5-mm sections and positioned on slides in fresh xylene for 15 min. Subsequently, the slides were hydrated through ethanol solutions and 2× saline sodium citrate (SSC) for 1 min in each solution. The slides were then incubated with Proteinase K solution at 37 °C for 20 min and subsequently rinsed in phosphate-buffered saline (PBS). After dehydration, each slide was treated with 20 μL of Hyb/probe solution and incubated at 4 °C overnight, after which 100 μL of Hyb/probe solution was added to each, and a coverslip was promptly mounted using HybridSlip. The following day, the slides were washed in 2× SSC at 37 °C for 30 min. After incubation in the blocking buffer, the slides were treated with an anti-digoxigenin antibody in a humid chamber at 37 °C for 60 min, followed by treatment with NBT: BCIP and staining with nuclear fast red. The experimental steps of IHC and ISH were the same as in our previous study [22].

Exosome isolation and characterization

The cell lines were cultured in normal medium until 60–70% confluence, thereafter, the medium was replaced with fresh medium supplemented with 10% exosome-depleted FBS. Then, the cell culture medium was harvested after 48 h and centrifuged (Beckman Coulter, Brea, CA, USA) at 2,000×g for 30 min at 4 °C to remove residual cells, debris and remaining macropolymers. The supernatant was passed through a 0.22-μm filter (Millipore, Danvers, MA, USA). After centrifugation at 3,000×g for 30 min at 4 °C in a dialysis tube (Millipore), the supernatant was incubated with ExoQuick-TC™ exosome precipitation solution (System Biosciences, Palo Alto, CA, USA) for 6 h to overnight at 4 °C. Subsequently, the mixture was centrifuged at 1,500×g for 30 min at 4 °C to harvest the yellow exosome pellets. The exosome pellets were resuspended in 100 μl phosphate-buffered saline (PBS) for further assays. Western blotting analysis was used to characterize the extracellular vesicle-associated protein markers Hsp70 (Abcam) and CD63 (Abcam) and the exosome-specific marker TSG101 (Abcam). For transmission electron microscopy (TEM), the exosomes were fixed with 1% glutaraldehyde, dropped in 300-mesh carbon/formvar-coated grids, stained with 2% uranyl acetate, dried and imaged by transmission electron microscopy (TEM) (FEI, Hillsboro, OR, USA), as previously reported [22]. The amount of exosomes was measured using the bicinchoninic acid (BCA) protein assay kit (Novagen, Merck Group, Madison, USA).

Exosome labelling and tracking

To monitor exosome trafficking, purified exosomes isolated from the culture medium were collected and labelled with PKH67 red fluorescent membrane linker dye (Sigma-Aldrich, Merck KGaA) according to the manufacturer's instructions. Next, the PKH26-labelled exosomes were washed and centrifuged at 100,000×g for 20 min at 4 °C to collect the exosomes, which were resuspended and added to unstained macrophages for exosome uptake studies. After treatment with PKH26-labelled exosomes for 4 h at 37 °C, the cells were detected by fluorescence microscopy.

RNA interference, vector transfection and qRT-PCR

The miR-205 mimic (10 nM), inhibitor (20 nM), negative control (10 nM) and PTEN expression plasmid (2 μg, GeneCopoeia) were transfected into cells using Lipofectamine 2000 reagent (Invitrogen) according to the manufacturer's protocol. The cells were collected for

further assays at 24–48 h after transfection. The transfection efficiencies were verified by fluorescence microscopy and RT-PCR analysis. Total RNA from cells and exosomes was extracted using TRIzol reagent (Invitrogen), and complementary DNA was synthesized with a reverse transcription system (GeneCopoeia, Guangzhou, China) according to the manufacturer's instructions. Reverse transcription and qRT-PCR were performed as previously described [22]. The relative expression levels were evaluated using the ΔΔCt method. The $2^{-\Delta\Delta Ct}$ method was applied to analyse the results. The primers for miR-205 mimic, miR-205 inhibitor, miR-205 nc, CD163, CD68, IL-10, CCL18, IL-1β, TNF-α and PTEN (GeneCopoeia) are available in the Supplementary Table 1.

Plasmids, transient transfections and luciferase assays

An miR-205 promoter (420 bp) was amplified from the mouse genomic DNA template and inserted into a pGL3 vector (Promega Corporation, Madison, WI, USA). Reporter vectors carrying the miR-205 target site were constructed by synthesizing a 3'-untranslated region (UTR) fragment containing the predicted target sites (miRWalk) for PTEN cDNA, and subsequently inserting the PTEN cDNA fragment into the multiple cloning site of a pMIR-REPORT™ luciferase miRNA expression reporter vector (Ambion Life Technologies, Carlsbad, CA, USA). For the luciferase reporter assay, HO-8910 cells were seeded in 24-well plates and transfected with the indicated plasmids. Cells were harvested 36 h after transfection. Luciferase activity was measured using the Dual-Luciferase® Reporter Assay System (Promega Corporation).

Western blot analysis

Proteins extracted from cells or exosomes were lysed in RIPA lysis buffer supplemented with protease inhibitor and quantified using a BCA protein assay kit (Novagen, Merck Group, Madison, USA). Approximately 30 μg of protein lysates (from each sample) were separated on 10% SDS-PAGE gels and transferred onto polyvinylidene difluoride membranes (Millipore). The membranes were blocked with 5% blocking buffer overnight at 4 °C with primary antibodies, followed by incubation with a secondary antibody at room temperature. The primary antibodies included anti-CD63, anti-TSG101, anti-Hsp70, anti-E-cadherin, anti-vimentin, anti-PTEN, anti-mTOR, anti-p-mTOR, anti-AKT, anti-p-AKT, anti-4EBP1, anti-p-4EBP1 (Cell Signaling Technology, USA) and anti-α-tubulin (Proteintech, Chicago, USA). The chemiluminescence signal was detected using an enhanced chemiluminescence mixture (Sigma-Aldrich), and images were captured using a gel imaging system (Bio-Rad Laboratories, CA, USA).

Co-culture, cell migration and invasion assays

Before starting the assays, THP-1 cells (1×10^4) were seeded on the bottom chamber of 8-mm Transwell inserts (Corning, Sigma-Aldrich) with PMA (100 ng/ml) for 48 h. Then, the THP-1 cells were differentiated into M0 macrophages, and the supernatant was replaced with normal medium containing 10% FBS for 24 h to eliminate the effect of PMA. Tumour cells (5×10^5) were seeded on the upper side of the co-culture system before the co-culture assay. After treatment with miR-205-Exos or miR-205 mimic/NC/inhibitor (RiboBio, Guangzhou, China), M0 macrophages were co-cultured with HO-8910 cells. Cell migration and invasion assays were performed as previously described [21].

Animal experiments

All animal experiments were performed in accordance with the National Institutes of Health (NIH) Guidelines for the Care and Use of Laboratory Animals and according to the protocols approved by the Animal Care and Use Committee at CSU. Female BALB/c nude mice (4–5 weeks old, 18 ~ 20 g) were housed in a specific pathogen-free environment in the Animal Laboratory Unit of CSU and were randomly divided into two groups ($n = 6$/group). HO-8910 cells (1.5×10^6 cells) mixed with conditioned macrophages pretreated with NC-Exos or miR-205-Exos were injected intraperitoneally (i.p.) into different groups. The procedure of living animal bioluminescence imaging was described previously [21].

Statistical analysis

All experiments were performed in triplicate. Data are presented as the mean ± standard error of the mean (SEM). Differences between treated and control groups were analysed using Student's *t* test or one-way ANOVA. Survival curves were estimated using the Kaplan-Meier method, and the log-rank test was used to calculate differences between the curves. A P-value less than 0.05 was considered statistically significant. Statistical analyses were performed by GraphPad Prism 5.0 (GraphPad Software, Inc., La Jolla, CA, USA).

Results

The expression level of miR-205 is correlated with TAM infiltration in OC patients

Macrophages are among the most abundant immune-related cells recruited to the tumour site and play significant roles in the TME. M2 macrophages, which are believed to be the main phenotype of TAMs, promote the progression and metastasis of tumours. In this study, an anti-CD163 antibody was used to identify M2 macrophages via immunohistochemistry (IHC). Compared with that in normal tissues, the expression of CD163 was dramatically upregulated in primary

tumours and its expression was even higher in metastatic tumours (Fig. 1A and B). In addition, the upregulation of CD163 was associated with a poor prognosis for OC patients (Fig. 1C and D). Moreover, we found that CD163 expression levels were higher in OC specimens with high miR-205 expression than in those with low miR-205 expression (Fig. 1E). Moreover, Spearman's correlation analysis suggested a corresponding upregulation of miR-205 when CD163 expression was increased (Fig. 1F). These results suggest that miR-205 expression is associated with TAM infiltration. In addition, OC patients exhibiting a strong correlation between CD163 and miR-205 expression were found to have more advanced cancer stages (stages III-IV vs. stages I-II: 19

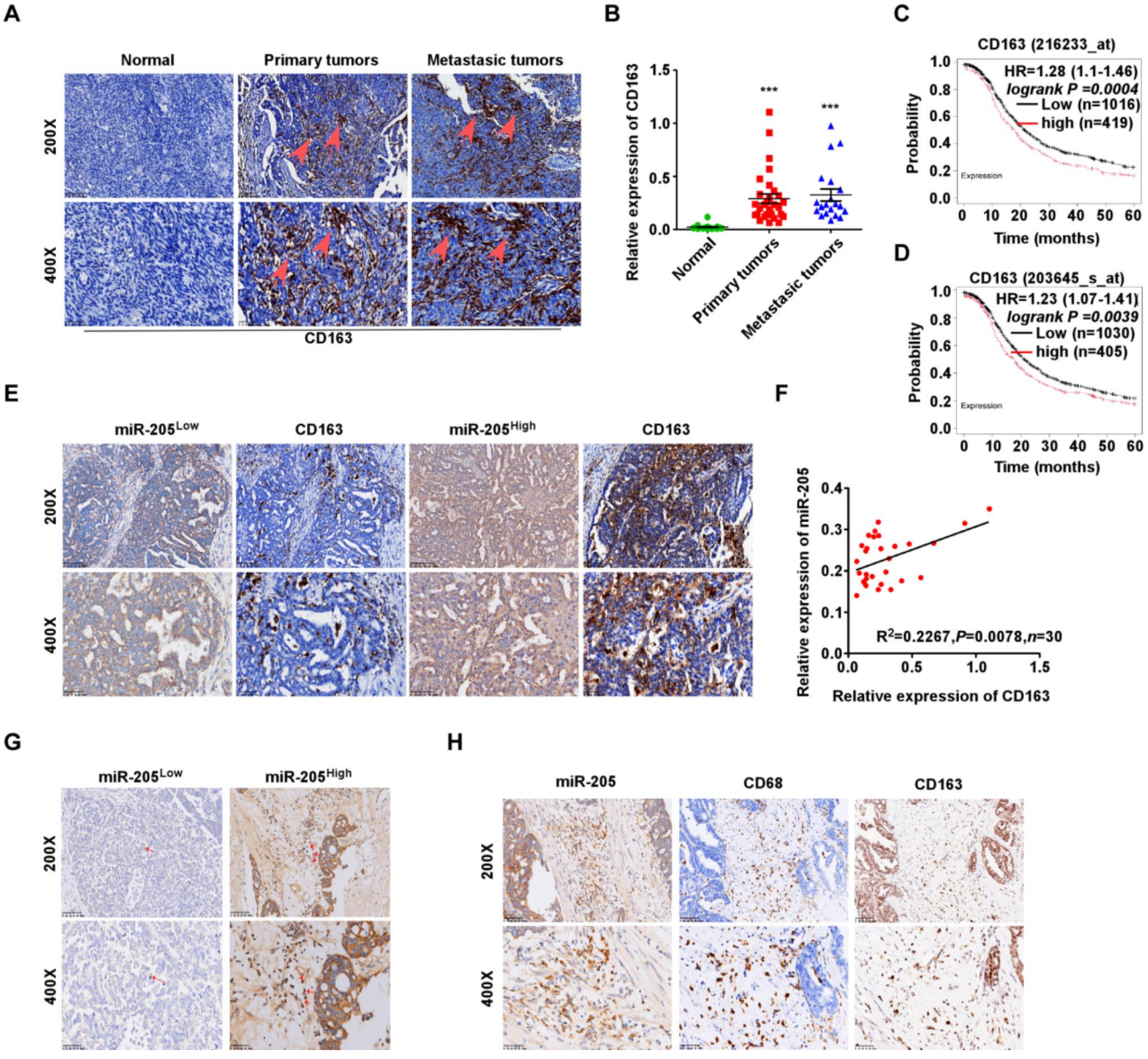

Fig. 1 miR-205 expression is associated with TAM infiltration in patients with OC. (**A**) IHC was used to detect the expression of the M2 marker CD163 in normal ovarian tissues, primary tumours and metastatic tumours. The red arrow indicates CD163-stained macrophages. Scale bar, 100 nm. (**B**) The relative expression of CD163 was determined for each group. (**C**, **D**) Kaplan–Meier curves for the overall survival of OC patients generated using the Kaplan–Meier Plotter database (www.kmplot.com). Red and black lines indicate patients with CD163 expression higher and lower than the median, respectively. The data are presented as the means ± SDs and were analysed with Student's *t* test. *** $P < < 0.001$.*** $P < 0.001$ (**E**) Representative images of IHC staining for CD163 in samples with high or low expression levels of miR-205. The cut-off for high expression was defined as values greater than the mean value, and for low expression, values less than the mean value were used as the cut-off. (**F**) Pearson correlation coefficient between miR-205 expression and CD163 expression in OC tissues. The Pearson correlation coefficient (r) and P value are shown, $n = 30$. (**G**) Representative images of miR-205 expression in OC tissues measured by ISH. The red arrow indicates macrophages. (**H**) Representative images of IHC staining for CD68 and CD163 in tissues with relatively high expression levels of miR-205. The scale bar in the 200× images represents 100 μm. The scale bar in the 400× images represents 50 μm

vs. 11) and higher drug resistance rates (77%). Interestingly, we found that high miR-205 expression in OC tissues was associated with the increased infiltration of miR-205-positive immune cells (Fig. 1G). Based on their morphology, we reasoned that the majority of the miR-205-positive immune cells observed in OC might be TAMs. We tested this hypothesis further by performing ISH and IHC to detect the expression of miR-205, the macrophage marker CD68, and the M2-type macrophage marker CD163 in the same two independent sets of OC samples. The following staining patterns were observed: miR-205 staining of both tumour cells and CD68 + and CD163 + cells in most of the OC tissue samples (31/54, Fig. 1H). Therefore, according to these results, we hypothesized that miR-205 expressed in OC cells may play an important role in macrophage polarization.

Exosomes from OC cells are able to polarize macrophages towards the M2 phenotype by transporting miR-205

The transfer of miRNAs by exosomes is especially interesting since exosomal miRNAs released from cancer cells can stimulate macrophages to switch their phenotype and play a role in promoting cancer progression and metastasis. Here, we investigated whether exosomal miR-205 derived from OC cells can be transported to macrophages and then reprogram the phenotype of TAMs. A model system was used to alter exosomal miR-205 expression and to reduce the effects of other factors present in the exosomes. The OC cell line HO-8910, which stably overexpresses miR-205, and a negative control cell line were established. Next, exosomes with relatively high miR-205 contents (miR-205-Exos) and relatively low miR-205 contents (NC-Exos) were isolated, and the expression of miR-205 was confirmed by qRT−PCR (Fig. 2A). As shown in Fig. 2B, the typical round particles ranged in diameter from 30 to 100 nm and were characterized by teacup-like shapes. Western blot analyses confirmed the presence of the exosomal proteins CD63, TSG101 and Hsp70 (Fig. 2C). After labelling with the fluorescent dye PKH67, miR-205-Exos from OC cells were incubated with macrophages. As shown in Fig. 2D, the PKH67-labelled exosomes could be internalized by macrophages. After treatment with exosomes, miR-205 expression was significantly increased in macrophages treated with the miR-205-Exos compared with those treated with the NC-Exos or the control (PBS) (Fig. 2E).

We assessed the immune phenotype and cytokine profile of macrophages that were differentiated from macrophage-like cells following exposure to exosomes to further investigate whether exosomal miR-205 alters the differentiation and function of macrophages. Human THP-1 monocytes were differentiated into macrophage-like cells by incubating them in the presence of phorbol 12-myristate 13-acetate (PMA), and these cells were characterized by an adherent morphology and the expression of the recognized macrophage marker CD68 (Fig. 2F-G). We assessed the possible role of exosomal miR-205 in macrophage polarization. The expression levels of M2 cytokines (CD163, IL-10 and CCL18) in macrophages were significantly increased when macrophage-like cells were incubated with miR-205-Exos compared with when they were incubated with NC-Exos or the control (Fig. 2H, I and J), whereas the expression of M1 cytokines (IL-1β and TNF-α) decreased significantly (Fig. 2K and L). Therefore, the above results demonstrate that exosomal miR-205 can promote the differentiation of macrophages into the M2 phenotype.

Tumour-derived exosomal miR-205 promotes OC cell migration and invasion by altering the polarization of M2-like macrophages in vitro

TAMs are widely known for their crucial roles in various aspects of cancer progression, including tumour cell invasion, motility, angiogenesis and premetastatic site formation. Next, a coculture system was established to investigate the effects of M2 macrophages induced by cancer-derived exosomal miR-205 on the migration, invasion and EMT of OC cells (Fig. 3A). After transfection with the miR-205 mimic or inhibitor, miR-205 was up- or downregulated, respectively, in OC cells (Fig. 3B). As shown in Fig. 3C and D, compared with NC-Exo-treated macrophages, miR-205-Exo-treated macrophages significantly increased the migration and invasion abilities of OC cells. Similarly, the downregulation of miR-205 in macrophages significantly enhanced the migration and invasion of OC cells (Fig. 3E and F), whereas the downregulation of miR-205 in macrophages weakened cell migration and invasion. Next, we sought to evaluate whether exosomal miR-205-induced macrophages affect the EMT in OC cells. After coculture with M2 macrophages induced by exosomal miR-205, the expression levels of an epithelial cell marker (E-cadherin) decreased, and the expression levels of mesenchymal cell markers (vimentin and MMP7) increased in OC cells. Similarly, the same results were obtained in the miR-205 mimic groups, and these effects were reversed by the miR-205 inhibitor (Fig. 3G and H). Taken together, these results suggest that exosomal miR-205-induced M2 macrophages could enhance the migration, invasion and EMT of OC cells.

Exosomal miR-205-induced M2 macrophages promote the development of OC in vivo

Next, we further evaluated the effects of exosomal miR-205-induced M2 phenotypic polarization on cancer progression. As shown in Fig. 4A, macrophages were

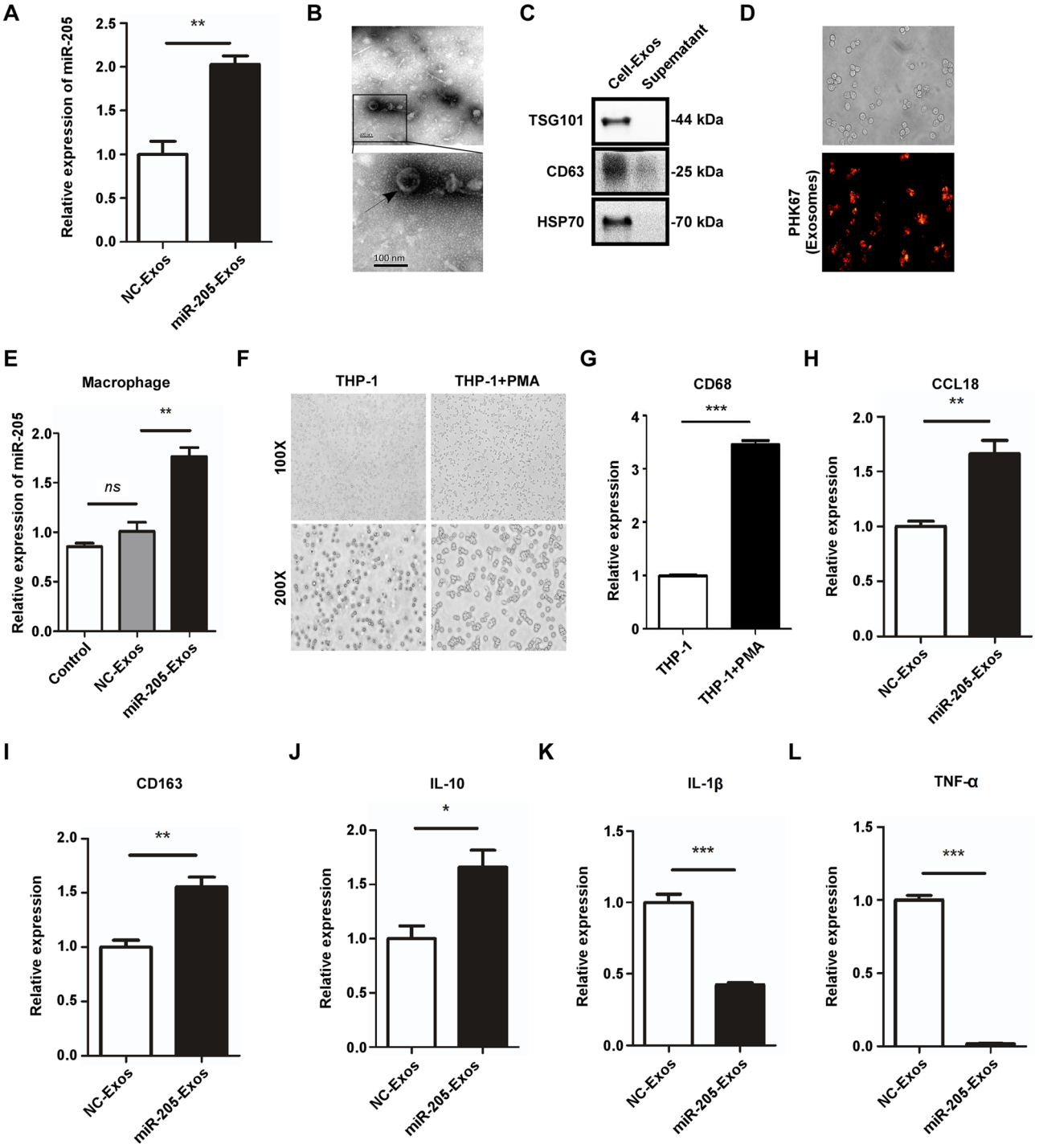

Fig. 2 Tumour-derived exosomes are able to induce M2-like macrophage polarization by transporting miR-205. (**A**) After treatment with the miR-205-Exos and NC-Exos, the miR-205 levels were measured by qRT–PCR. (**B**) Isolated exosomes were identified via electron microscopy (black arrows). Scale bar, 100 nm. (**C**) The exosome-specific marker TSG101 and the extracellular vesicle-related protein markers Hsp70 and CD63 were measured by Western blot analysis. Cell exosomes: exosomes isolated from the cell culture medium; supernatant: supernatant obtained after the last centrifugation. (**D**) Exosomes from HO-8910-miR-205 cells were labelled with PKH26 and then added to the macrophage culture medium. (**E**) After treatment with the miR-205-Exos, NC-Exos or the control (as a blank control), the miR-205 levels in the macrophages were measured by qRT–PCR. (**F**) THP-1 cells were treated with phorbol-12-myristate-13-acetate (PMA) for 24 h. (**G**) After treatment with PMA, the expression levels of CD68 in THP-1 cells were detected using qRT–PCR. (**H-J**) The effects of the miR-205-Exos and NC-Exos on the expression levels of M2-type markers (CD163, IL-10 and CCL18) in macrophages were analysed using qRT–PCR. (**K**, **L**) M1-type marker (IL-1β and TNF-α) levels were detected by qRT–PCR after treatment with the miR-205-Exos and NC-Exos. All the data are shown as the means ± SEMs from at least three independent experiments. *$P < 0.05$, **$P < 0.01$ and ***$P < 0.001$, Student's *t* test. *n.s.*, not significant

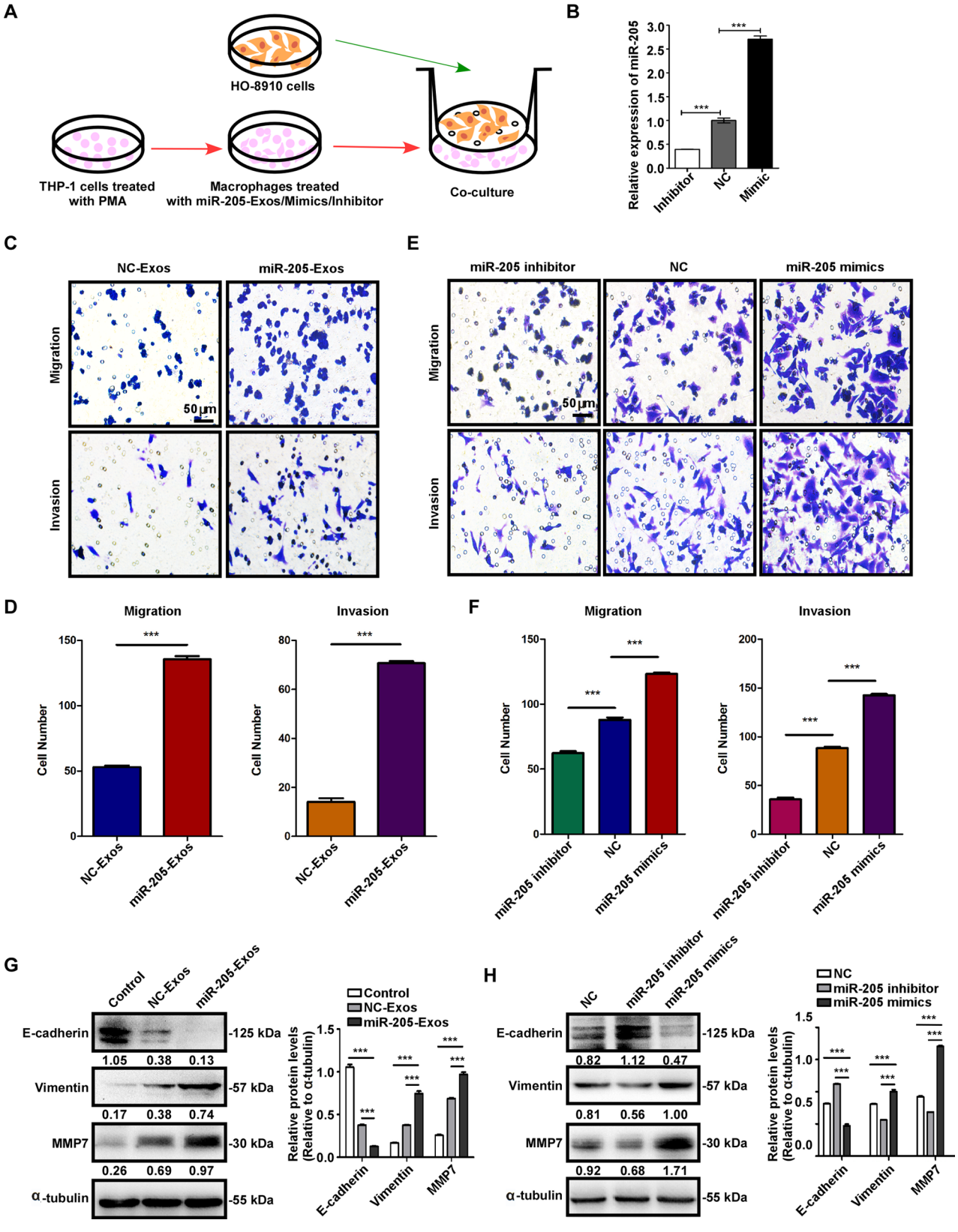

Fig. 3 (See legend on next page.)

(See figure on previous page.)

Fig. 3 Exosomal miR-205-induced M2 macrophages enhanced cancer cell migration, invasion, and the EMT. (**A**) Schematic illustration of the in vitro indirect coculture system. (**B**) After treatment with the miR-205 inhibitor, NC or mimics, the miR-205 levels in the macrophages were measured by qRT–PCR. (**C**, **D**) The migration and invasion of OC cells (HO-8910) cocultured with macrophages treated with exosomes (miR-205-Exos, NC-Exos and control (as a blank control)) or rmiR-205 mimics/NC/inhibitors was determined using an in vitro Transwell coculture system. Representative images of migratory or invading cells on membranes coated with or without Matrigel are shown. The scale bar represents 50 μm. (**E**, **F**) Morphometric analysis of migratory and invasive cells. (**G**, **H**) The effects of the supernatants of macrophages treated with exosomes or rmiR-205 mimics/NC/inhibitors on the EMT of HO-8910 cells were analysed by Western blotting. All the data are shown as the means ± SEMs from at least three independent experiments. ***$P < 0.001$, Student's *t* test

pretreated with NC-Exos or miR-205-Exos for 48 h. Then, luciferase-labelled HO-8910 cells mixed with the pretreated macrophages were injected into the abdominal cavities of nude mice. The mice were subsequently intraperitoneally injected with the same number of macrophages pretreated with NC-Exos or miR-205-Exos every three days. An IVIS system was used to detect luciferase activity levels, which reflect the tumour volume in the peritoneal cavity. Compared with those in the NC-Exo group, the luciferase activity levels in the miR-205-Exo group increased significantly, especially at three and four weeks after the first injection (Fig. 4B and C). In addition, the number of peritoneal implants in the miR-205-Exo group was greater than that in the NC-Exo group (Fig. 4D). Compared with the mice in the NC-Exo group, the mice in the miR-205-Exo group experienced shorter survival times (Fig. 4E). IHC and HE staining revealed that the expression levels of CD163 (an M2-type macrophage marker) were significantly increased in the miR-205-Exo group compared with the NC-Exo group (Fig. 4F and G), suggesting that more M2 macrophages infiltrated the cancer tissues in the miR-205-Exo group than in the NC-Exo group. These results indicate that exosomal miR-205 induces the M2-type polarization of macrophages in the TME and promotes cancer progression in vivo.

Exosomal miR-205 polarized M2 macrophages via activation of the PI3K/AKT/mTOR axis

TargetScan and miRBase were used to identify possible miR-205 target genes and explore the mechanism by which exosomal miR-205 modulates macrophage polarization in detail. The candidate target gene PTEN was chosen for its role in the regulation of macrophage polarization [26], and luciferase reporter assays were performed to confirm the direct inhibitory effect of miR-205 on PTEN (Fig. 5A). Consistent with the results of the luciferase reporter analysis, the miR-205 mimics or the miR-205-Exos significantly decreased the PTEN mRNA and protein levels in the macrophages, whereas the miR-205 inhibitor had the opposite effects (Fig. 5B and C). As shown in Fig. 5D and E, the expression level of PTEN that was suppressed by miR-205 or miR-205-Exos in macrophages was rescued by with the transfection of a PTEN plasmid. Furthermore, the role of PTEN in miR-205-induced macrophage polarization and cytokine production was investigated using PTEN plasmid, miR-205 and miR-205-Exos. Consistent with the findings described above, the overexpression of miR-205 notably increased the expression levels of M2-type markers (CD163 and IL-10) (Fig. 5F-I) and decreased the levels of M1-type markers (IL-1β and TNF-α) (Fig. 5J-M), and these effects were reversed by PTEN expression.

PTEN is a negative regulator of the PI3K pathway and has been shown to reprogram tumour-infiltrating macrophages. We next examined whether exosomal miR-205 regulates macrophage polarization through the PTEN/PI3K/AKT/mTOR axis. Notably, treatment with the miR-205 mimics or the miR-205-Exos resulted in significantly decreased expression of PTEN and increased expression levels of p-AKT, p-mTOR and p-4EBP-1 in macrophages,

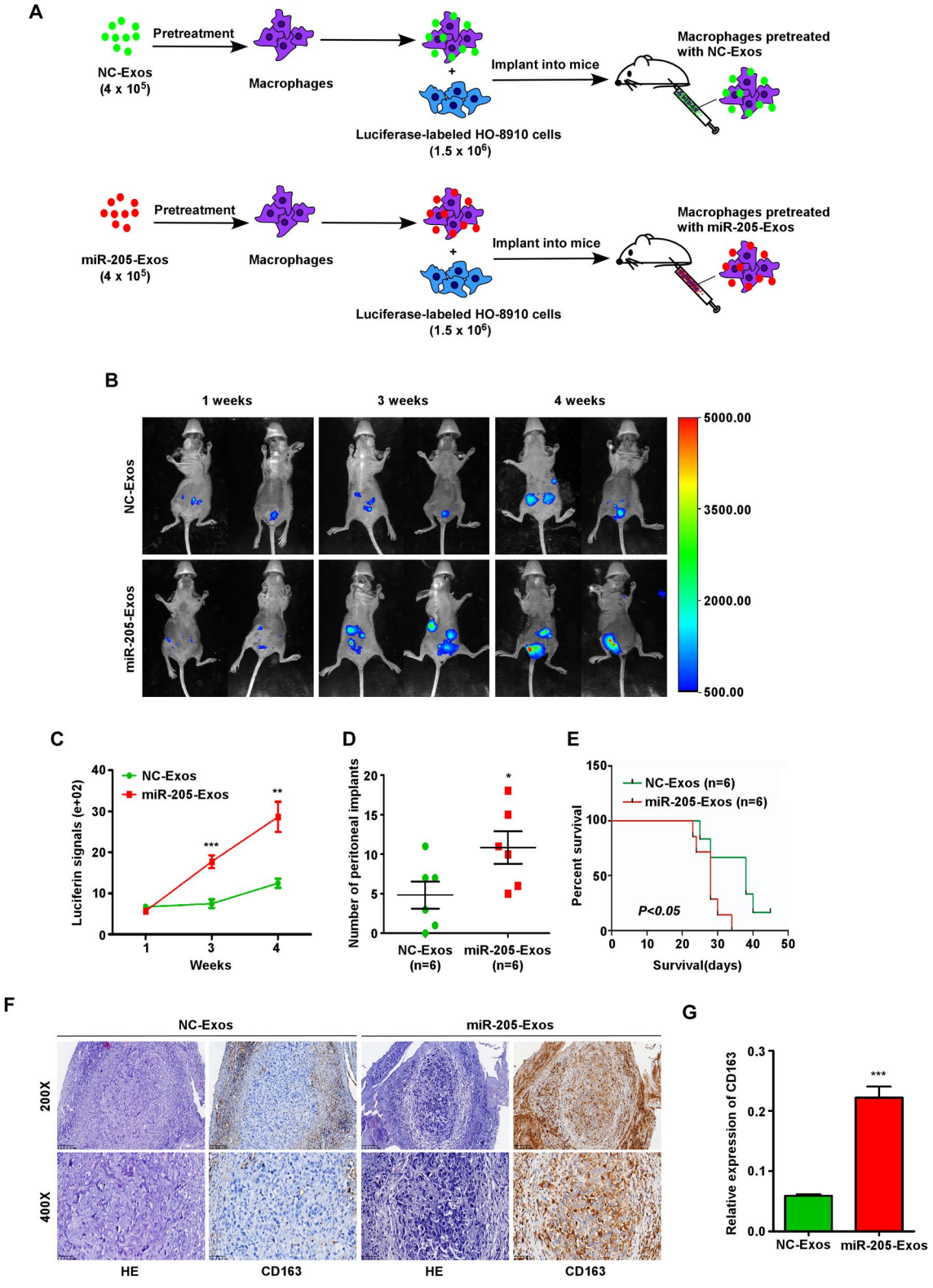

Fig. 4 (See legend on next page.)

(See figure on previous page.)

Fig. 4 Tumour-derived exosomal miR-205 promotes OC progression in vivo. (**A**) Macrophages pretreated with miR-205-Exos or NC-Exos were mixed with luciferase-labelled HO-8910 cells, and then the mixtures were injected into the abdominal cavities of nude mice ($n=6$ each). Thereafter, macrophages pretreated with exosomes were injected into the abdominal cavities of the mice every 5 days. (**B**) Representative images of mice at different time points between 1 week and 4 weeks (from left to right) after the injection of the mixtures. After an i.p. injection of 100 mg/kg D-luciferin, the mice were anaesthetized with 2.0% isoflurane and imaged using the IVIS system every week. The colour bars represent the tumour cell intensity from low (blue) to high (red). (**C**) Luciferase activities of the peritoneal tumours were measured every week. (**D**) The number of peritoneal tumour implants in each indicated group. (**E**) The survival status of each mouse was recorded daily. Kaplan–Meier analysis was performed to analyse the overall survival rates of the nude mice in the indicated groups. (**F**, **G**) Mouse xenografts were subjected to HE and IHC staining for CD163, and the relative expression of CD163 was quantitatively assessed. The data are presented as the means ± SEMs; $^{*}P<0.05$, $^{**}P<0.01$, and $^{***}P<0.001$

and these effects were reversed by PTEN expression (Fig. 6A and B). We then evaluated the effect of specific blockade of the PI3K/AKT/mTOR signalling pathway on M2 macrophage polarization induced by exosomal miR-205. Western blot analyses confirmed that the PI3K inhibitor GDC-0941, the AKT inhibitor MK-2206 and the mTOR inhibitor rapamycin effectively blocked the activation of the PI3K/AKT/mTOR pathway induced by miR-205 upregulation (Fig. 6C). As shown in Fig. 6D-K, the effects of miR-205 overexpression on M2 macrophage polarization were significantly abolished by GDC-0941, MK-2206 and rapamycin. These data indicate that exosomal miR-205 activates the PI3K/AKT/mTOR axis by downregulating PTEN expression in macrophages, thus inducing the polarization of macrophages towards the M2 phenotype.

Discussion

With the increasing popularity of clinical immunotherapy in recent years, the regulation of the immune microenvironment in OC has garnered increasing attention [27, 28]. The tumour microenvironment, particularly the presence and polarization of TAMs, plays a critical role in the progression and metastasis of ovarian cancer by influencing tumour growth and modulating immune responses [29–31]. Many studies have reported that the communication between cancer cells and macrophages can be mediated by exosomes and that exosomal miRNAs released from cancer cells can reprogram macrophages to establish a type of immunosuppressive tumour microenvironment that may promote the invasion and metastasis of tumour cells [32, 33].

Our study focused on elucidating the molecular mechanisms through which miR-205 mediates the polarization of TAMs towards the M2 phenotype within the ovarian cancer microenvironment. Research has suggested that miRNAs significantly regulate the interactions between tumour cells and immune cells; however, the specific role of miR-205 in ovarian cancer remains poorly defined. Here, we present key findings showing that exosomal miR-205 derived from OC cells can induce the M2 polarization of macrophages, thereby promoting tumour progression in vitro and in vivo. The activation of the PI3K/AKT/mTOR signalling pathway in this context further underscores the potential of targeting miR-205 as a therapeutic strategy in ovarian cancer management (Scheme 1).

Exosomes are important components of the TME and act as important messengers that mediate the cross-talk between tumour cells and immune cells [33, 34]. Numerous studies have suggested that exosomal miRNAs can significantly influence the phenotypic transformation of

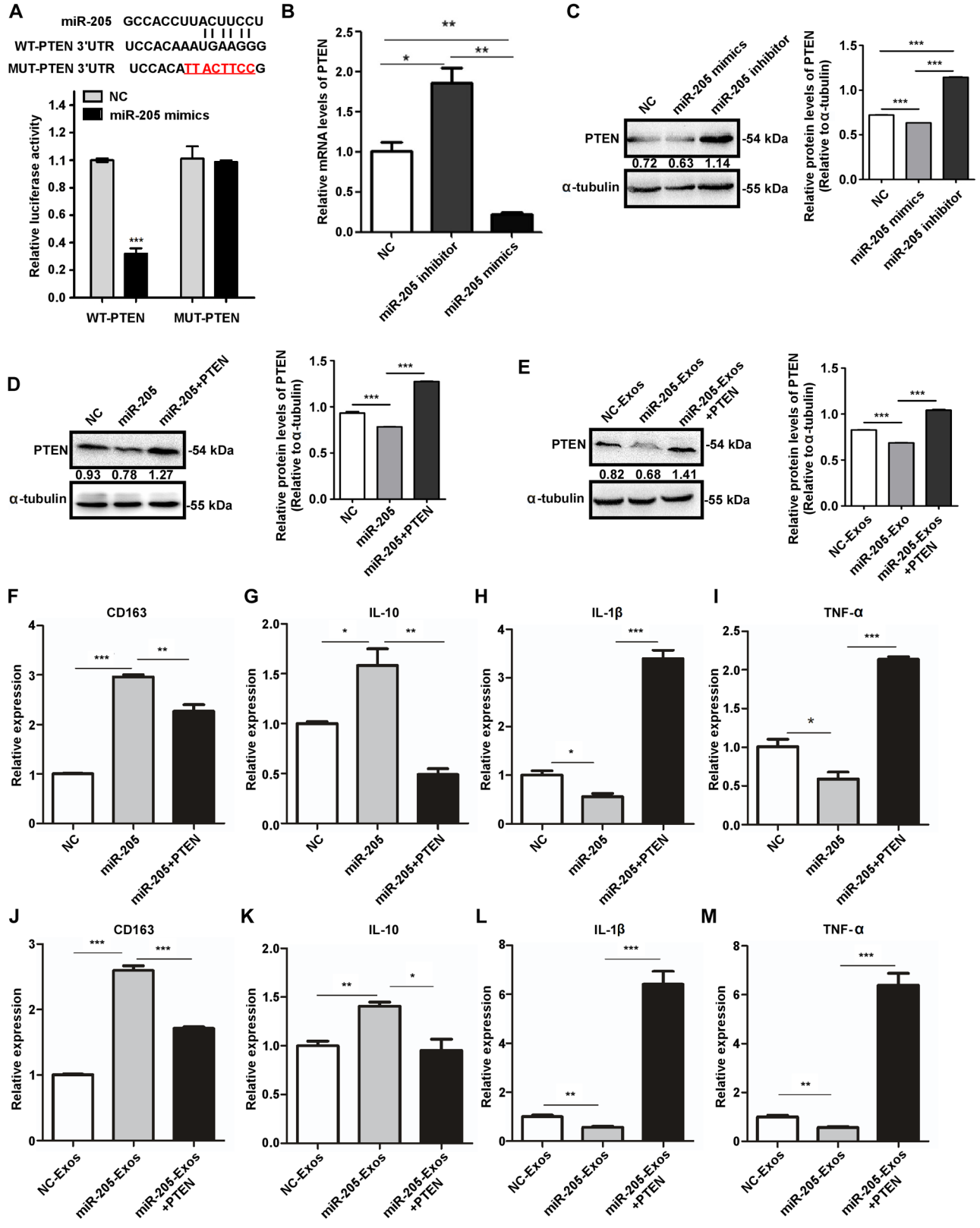

Fig. 5 (See legend on next page.)

(See figure on previous page.)

Fig. 5 Exosomal miR-205 regulates M2 macrophage polarization by targeting PTEN. (**A**) Putative target sites for miR-205 in the 3′ UTR of PTEN. The target sequence of the PTEN 3′ UTR was mutated. After transfection with the wild-type or mutant reporter PTEN plasmid, the luciferase activity was analysed using the dual-luciferase reporter assay system. (**B**) After treatment with the miR-205 inhibitor, NC or mimic, the PTEN mRNA levels in the macrophages were measured by qRT–PCR. (**C**) The protein expression of PTEN in macrophages after treatment with the miR-205 inhibitor, NC or mimics was assessed by Western blotting. (**D**) Western blotting was used to detect PTEN and α-tubulin levels in macrophages incubated with NC, miR-205 or miR-205 + PTEN. (**E**) Western blotting was used to detect PTEN and α-tubulin levels in macrophages incubated with NC-Exos, miR-205-Exos or miR-205-Exos + PTEN. (**F-M**) The effects of NC, miR-205, miR-205 + PTEN, NC-Exos, miR-205-Exos and miR-205-Exos + PTEN on the expression levels of M1-type (IL-1β and TNF-α) and M2-type (CD163 and IL-10) markers in macrophages were analysed by qRT–PCR. All the experiments were repeated three times, and the results are presented as the means ± SEMs. Statistical significance was determined using a two-tailed, unpaired Student's *t* test. *$P < 0.05$, **$P < 0.01$ and ***$P < 0.001$

macrophages through various targets [35, 36]. Moreover, the release of exosomal miRNAs from cancer cells promotes tumour progression [37]. The findings of this study highlight the critical role of tumour-associated macrophages (TAMs) in ovarian cancer (OC) progression, with a particular focus on the modulation of miR-205 in the tumour microenvironment. Our results demonstrate that exosomes derived from OC cells significantly influence macrophage polarization towards the M2 phenotype, which is associated with increased tumour growth and metastasis. This polarization is mediated by the activation of the PTEN-PI3K/AKT/mTOR pathway, underscoring the importance of miR-205 as a potential therapeutic target in OC. Previous studies have established a link between TAMs and tumour progression, particularly in terms of how M2 macrophages contribute to immune evasion and promote the formation of a microenvironment that is favourable for tumour growth [38–41]. Moreover, the modulation of miR-205 expression in this context suggests that targeting this microRNA may represent a novel approach to reprogram the tumour microenvironment and increase the efficacy of existing therapies.

Additionally, the results suggest that the activation of the PI3K/AKT/mTOR signalling pathway by miR-205 is critical for the M2 polarization of macrophages, which plays a significant role in OC progression. These findings align with the findings from other studies indicating that the PI3K/AKT pathway is crucial for macrophage differentiation and function, particularly in cancer settings [26, 42–48]. The dysregulation of this signalling pathway in TAMs may not only contribute to the immunosuppressive tumour microenvironment but also facilitate the aggressive behaviour of OC cells. Furthermore, our study revealed that high levels of miR-205 correlate with increased levels of M2 markers in macrophages, providing insights into potential biomarkers for disease progression and therapeutic targets for intervention.

This study is not without its limitations. The relatively small sample size may hinder the generalizability of the findings, as it does not fully represent the heterogeneity observed in ovarian cancer patient populations. Furthermore, the lack of comprehensive clinical validation limits the ability to draw robust conclusions regarding the translational potential of miR-205 as a therapeutic target. Additionally, while the focus on macrophage polarization provides important insights, the functional differences among various macrophage subtypes have not been extensively explored, which may obscure a complete understanding of their roles in the tumour microenvironment. Potential batch effects during data analysis could also introduce variability, affecting the reliability of the results.

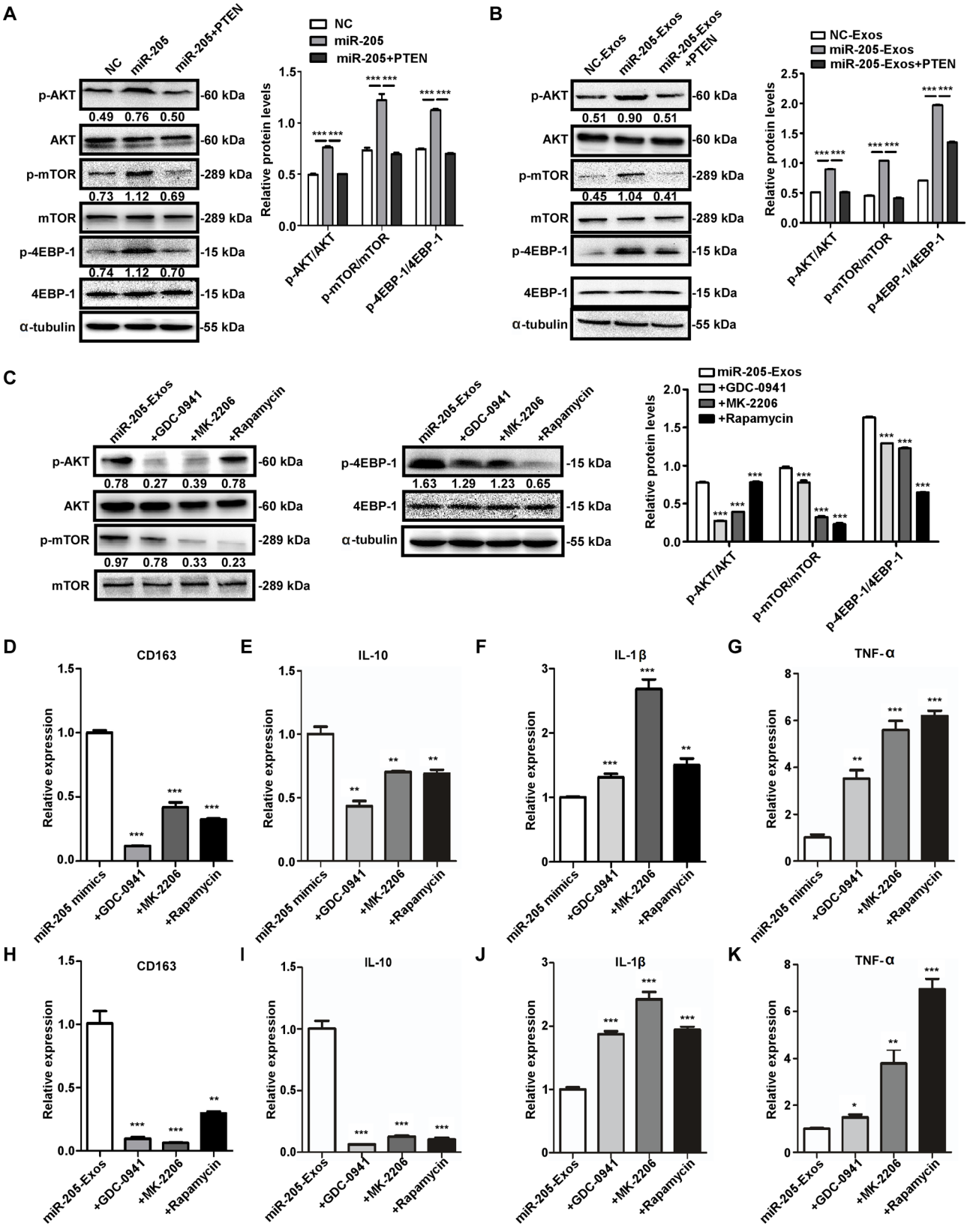

Fig. 6 (See legend on next page.)

(See figure on previous page.)

Fig. 6 miR-205 regulates macrophage polarization by activating the PTEN-PI3K/AKT/mTOR signalling pathway. (**A**) After the cells were transfected with NC, miR-205 or miR-205 + PTEN, p-AKT, AKT, p-mTOR, mTOR, p-4EBP-1, 4EBP-1 and α-tubulin levels in the macrophages were detected via Western blotting. (**B**) After an incubation with NC-Exos, miR-205-Exos or miR-205-Exos + PTEN, Western blotting was performed to detect PTEN, p-AKT, AKT, p-mTOR, mTOR, p-4EBP-1, 4EBP-1 and α-tubulin levels in macrophages. (**C**) Western blot analysis showing the effects of miR-205-Exos, miR-205-Exos + GDC-0941, miR-205-Exos + MK-2206 and miR-205-Exos + rapamycin on the protein levels of p-AKT, AKT, p-mTOR, mTOR, p-4EBP-1, 4EBP-1 and α-tubulin. (**D-G**) After the cells were transfected with the miR-205 mimics, the effects of GDC-0941, MK-2206 and rapamycin on the expression levels of M1-type (IL-1β and TNF-α) and M2-type (CD163 and IL-10) markers were analysed by qRT–PCR. (**H-K**) After an incubation with miR-205-Exos, the effects of GDC-0941, MK-2206 and rapamycin on M1-type (IL-1β and TNF-α) and M2-type (CD163 and IL-10) marker expression levels were analysed by qRT–PCR. All the experiments were repeated three times, and the results are presented as the means ± SEMs. Statistical significance was determined using a two-tailed, unpaired Student's *t* test. **P* < 0.05, ***P* < 0.01 and ****P* < 0.001. n.s., not significant

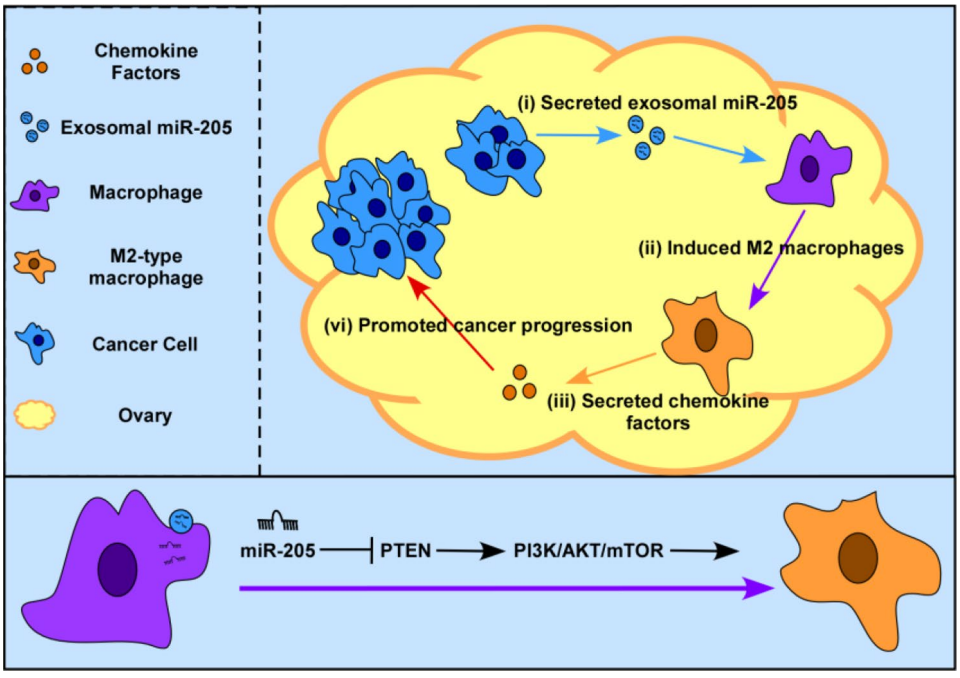

Scheme 1 Schematic diagram of the role of tumour-derived exosomal miR-205 in M2 macrophage polarization during cancer progression

Addressing these limitations in future studies is crucial to enhance the validity and applicability of the findings.

Conclusions

In conclusion, this research elucidates the molecular mechanisms by which miR-205 modulates macrophage polarization through extracellular vesicles within the ovarian cancer microenvironment. These findings underscore the critical role of miR-205 in tumour progression and highlight its potential as a therapeutic target. By providing new insights into the dynamic interplay between tumour cells and immune cells, this study lays the groundwork for future investigations aimed at developing innovative strategies for ovarian cancer treatment. Continued exploration of miR-205 and its regulatory pathways may ultimately contribute to improved therapeutic outcomes and a deeper understanding of cancer immunobiology.

Abbreviations

CD163	Macrophage mannose receptors 163
CD68	Cluster of Differentiation 68
CCL18	chemokine (C-C motif) ligand 18
EMT	Epithelial-mesenchymal transition
FBS	Foetal bovine serum
ISH	In situ hybridization
IHC	Immunohistochemistry
miRNAs	MicroRNAs
IL-6	Interleukin-6
IL-1β	Interleukin-1β
IL-10	Interleukin-10
IOD	Integral optical density
miRNAs	MicroRNAs
OC	Ovarian cancer
PBS	Phosphate-buffered saline
PMA	Phorbol 12-myristate 13-acetate
TEM	Transmission electron microscopy
TAMs	Tumour-associated macrophages
TME	Tumour microenvironment
TNF-α	Tumor necrosis factor-α

Supplementary Information

The online version contains supplementary material available at https://doi.org/10.1186/s13048-025-01616-3.

Supplementary Material 1

Acknowledgements
Not applicable.

Author contributions
LQH conceived, designed the study, prepared all the figures and wrote the manuscript. QC contributed to the study design and performed the experiments. XYW contributed to the study design and reviewed and edited the manuscript. All authors read and approved the final manuscript.

Funding
This work was supported by grants from the National Natural Science Foundation of China (grant no. 81172469), the Open Sharing Fund for the Large-scale Instruments and Equipments of Central South University (grant no. CSUZC202039), the Scientific Research Launch Project for new employees of the Second Xiangya Hospital of Central South University, Changshashi Natural Science Foundation of China (2022) (grant no. kq2208300), National Health Service Research of Hunan Province of China (grant no. W20243157), and Hunan Provincial Natural Science Foundation of China (grant no. 2019JJ40394 and 2022JJ40687).

Data availability
No datasets were generated or analysed during the current study.

Declarations

Ethics approval and consent to participate
The present study was approved by the Ethics Committee of Xiangya Hospital (Central South University, Changsha, China) and conducted in adherence with the Declaration of Helsinki. The patients were informed about the sample collection and had signed informed consent forms.

Competing interests
The authors declare no competing interests.

Received: 22 October 2024 / Accepted: 1 February 2025
Published online: 15 February 2025

References

1. Torre LA, Trabert B, DeSantis CE, Miller KD, Samimi G, Runowicz CD, Gaudet MM, Jemal A, Siegel RL. Ovarian cancer statistics, 2018, CA: a cancer journal for clinicians, 68 (2018) 284–96.
2. Miller KD, Nogueira L, Devasia T, Mariotto AB, Yabroff KR, Jemal A, Kramer J, Siegel RL. Cancer treatment and survivorship statistics, 2022. CA Cancer J Clin. 2022;72(5):409–36.
3. Bhat BA, Saifi I, Khamjan NA, Hamdani SS, Algaissi A, Rashid S, Alshehri MM, Ganie SA, Lohani M, Abdelwahab SI, Dar SA. Exploring the tumor immune microenvironment in ovarian cancer: a way-out to the therapeutic roadmap. Expert Opin Ther Targets. 2023;27:841–60.
4. Garlisi B, Lauks S, Aitken C, Ogilvie LM, Lockington C, Petrik D, Eichhorn JS, Petrik J. The Complex Tumor Microenvironment in Ovarian Cancer: therapeutic challenges and opportunities. Curr Oncol. 2024;31:3826–44.
5. Kelliher L, Lengyel E. Understanding long-term survival of patients with ovarian Cancer-the Tumor Microenvironment comes to the Forefront. Cancer Res. 2023;83:1383–5.
6. Tavira B, Iscar T, Manso L, Santaballa A, Gil-Martin M, Garcia Garcia Y, Romeo M, Iglesias M, de Juan Ferre A, Barretina-Ginesta MP, Manzano A, Gaba L, Rubio MJ, de Andrea CE. A. Gonzalez-Martin, Analysis of Tumor Microenvironment Changes after Neoadjuvant Chemotherapy with or without Bevacizumab in Advanced Ovarian Cancer (GEICO-89T/MINOVA study), clinical cancer research. Volume 30. an official journal of the American Association for Cancer Research; 2024. pp. 176–86.
7. Shu H, Lv W, Ren ZJ, Li H, Dong T, Zhang Y, Nie F. Ultrasound-mediated PLGA-PEI nanobubbles carrying STAT6 SiRNA enhances NSCLC Treatment via Repolarizing Tumor-associated macrophages from M2 to M1 phenotypes. Curr Drug Deliv. 2024;21:1114–27.
8. Hadimani SM, Das S, Harish KG. An immunohistochemical evaluation of tumor-associated macrophages (M1 and M2) in carcinoma prostate - an institutional study. J Cancer Res Ther. 2023;19:S300–5.
9. Yang B, Li G, Wang S, Zheng Y, Zhang J, Pan B, Wang N, Wang Z. Tumor-associated macrophages/C-X-C motif chemokine ligand 1 promotes breast cancer autophagy-mediated chemoresistance via IGF1R/STAT3/HMGB1 signaling. Cell Death Dis. 2024;15:743–58.
10. Wei Y, Li R, Wang Y, Fu J, Liu J, Ma X. Nanomedicines Targeting Tumor cells or Tumor-Associated macrophages for Combinatorial Cancer Photodynamic Therapy and Immunotherapy: strategies and influencing factors. Int J Nanomed. 2024;19:10129–44.
11. Bui I, Bonavida B. Polarization of M2 Tumor-Associated macrophages (TAMs) in Cancer Immunotherapy. Crit Rev Oncog. 2024;29:75–95.
12. Wang D, Wang X, Si M, Yang J, Sun S, Wu H, Cui S, Qu X, Yu X. Exosome-encapsulated miRNAs contribute to CXCL12/CXCR4-induced liver metastasis of colorectal cancer by enhancing M2 polarization of macrophages. Cancer Lett. 2020;474:36–52.
13. Theodoraki MN, Huber D, Hofmann L, Werner L, Idel C, Fleckner J, Plotze-Martin K, Schutt L, Brunner C, Depping R, Hoffmann TK, Bruchhage KL, Pries R. Type 2-like polarization and elevated CXCL4 secretion of monocyte derived macrophages upon internalization of plasma-derived exosomes from head and neck cancer patients. BMC Cancer. 2024;24:1173–85.
14. Lu Y, Zheng J, Lin P, Lin Y, Zheng Y, Mai Z, Chen X, Xia T, Zhao X, Cui L. Tumor Microenvironment-Derived exosomes: a double-edged Sword for Advanced T cell-based immunotherapy. ACS Nano. 2024;18:27230–60.
15. Liu J, Zhao H, Gao T, Huang X, Liu S, Liu M, Mu W, Liang S, Fu S, Yuan S, Yang Q, Gu P, Li N, Ma Q, Liu J, Zhang X, Zhang N, Liu Y. Glypican-3-targeted macrophages delivering drug-loaded exosomes offer efficient cytotherapy in mouse models of solid tumours. Nat Commun. 2024;15:8203–23.
16. Gong X, Zhao Q, Zhang H, Liu R, Wu J, Zhang N, Zou Y, Zhao W, Huo R, Cui R. The effects of mesenchymal stem cells-derived exosomes on metabolic reprogramming in scar formation and Wound Healing. Int J Nanomed. 2024;19:9871–87.
17. Liao Z, Chen Y, Duan C, Zhu K, Huang R, Zhao H, Hintze M, Pu Q, Yuan Z, Lv L, Chen H, Lai B, Feng S, Qi X, Cai D. Cardiac telocytes inhibit cardiac microvascular endothelial cell apoptosis through exosomal miRNA-21-5p-targeted cdip1 silencing to improve angiogenesis following myocardial infarction. Theranostics. 2021;11:268–91.
18. Razo-Azamar M, Nambo-Venegas R, Quevedo IR, Juarez-Luna G, Salomon C, Guevara-Cruz M, Palacios-Gonzalez B. Early-pregnancy serum maternal and placenta-derived exosomes miRNAs Vary based on pancreatic beta-cell function in GDM. J Clin Endocrinol Metab. 2024;109:1526–39.
19. Zhou Y, Zhang Y, Xu J, Wang Y, Yang Y, Wang W, Gu A, Han B, Shurin GV, Zhong R, Shurin MR, Zhong H. Schwann cell-derived exosomes promote lung cancer progression via miRNA-21-5p. Glia. 2024;72:692–707.
20. Tong F, Mao X, Zhang S, Xie H, Yan B, Wang B, Sun J, Wei L. HPV + HNSCC-derived exosomal miR-9 induces macrophage M1 polarization and increases tumor radiosensitivity. Cancer Lett. 2020;478:34–44.
21. Li J, Hu K, Gong G, Zhu D, Wang Y, Liu H, Wu X. Upregulation of MiR-205 transcriptionally suppresses SMAD4 and PTEN and contributes to human ovarian cancer progression. Sci Rep. 2017;7:41330–9.
22. He L, Zhu W, Chen Q, Yuan Y, Wang Y, Wang J, Wu X. Ovarian cancer cell-secreted exosomal miR-205 promotes metastasis by inducing angiogenesis. Theranostics. 2019;9:8206–20.
23. Xiong J, He X, Xu Y, Zhang W, Fu F. MiR-200b is upregulated in plasma-derived exosomes and functions as an oncogene by promoting macrophage M2 polarization in ovarian cancer. J Ovarian Res. 2021;14:74–84.
24. Chen X, Zhou J, Li X, et al. Exosomes derived from hypoxic epithelial ovarian cancer cells deliver microRNAs to macrophages and elicit a tumor-promoted phenotype. Cancer Lett. 2018;435:80–91.
25. Zhou J, Li X, Wu X, et al. Exosomes released from Tumor-Associated macrophages transfer miRNAs that induce a Treg/Th17 Cell Imbalance in Epithelial Ovarian Cancer. Cancer Immunol Res. 2018;6:1578–92.
26. Chen T, Liu Y, Li C, Xu C, Ding C, Chen J, Zhao J. Tumor-derived exosomal circFARSA mediates M2 macrophage polarization via the PTEN/PI3K/AKT pathway to promote non-small cell lung cancer metastasis. Cancer Treat Res Commun. 2021;28:100412–20.
27. Yeh CY, Aguirre K, Laveroni O, Kim S, Wang A, Liang B, Zhang X, Han LM, Valbuena R, Bassik MC, Kim YM, Plevritis SK, Snyder MP, Howitt BE, Jerby L. Mapping spatial organization and genetic cell-state regulators to target immune evasion in ovarian cancer. Nat Immunol. 2024;25:1943–58.
28. Nguyen LL, Watson ZL, Ortega R, Woodruff ER, Jordan KR, Iwanaga R, Yamamoto TM, Bailey CA, To F, Jeong AD, Guntupalli SR, Behbakht K, Gibaja V, Arnoult N, Cocozaki A, Chuong EB, Bitler BG. Combining EHMT and PARP Inhibition: A Strategy to Diminish Therapy-Resistant Ovarian Cancer Tumor

Growth while Stimulating Immune Activation, Molecular cancer therapeutics, (2024) OF1-OF16.
29. Cruz LS, Robinson M, Stevenson D, Amador IC, Jordan GJ, Valencia S, Navarrete C, House CD. Chemotherapy enriches for proinflammatory macrophage phenotypes that support Cancer Stem-Like cells and Disease Progression in Ovarian Cancer. Cancer Res Commun. 2024;4:2638–52.
30. Gao J, Zhao Z, Pan H, Huang Y. Significance of dysregulated M2 macrophage and ESR2 in the ovarian metastasis of gastric cancer. Translational cancer Res. 2024;13:2674–90.
31. Puttock EH, Tyler EJ, Manni M, Maniati E, Butterworth C, Burger Ramos M, Peerani E, Hirani P, Gauthier V, Liu Y, Maniscalco G, Rajeeve V, Cutillas P, Trevisan C, Pozzobon M, Lockley M, Rastrick J, Laubli H, White A, Pearce OMT. Extracellular matrix educates an immunoregulatory tumor macrophage phenotype found in ovarian cancer metastasis. Nat Commun. 2023;14:2514–30.
32. Wang F, Niu Y, Chen K, Yuan X, Qin Y, Zheng F, Cui Z, Lu W, Wu Y, Xia D. Extracellular vesicle-packaged circATP2B4 mediates M2 macrophage polarization via miR-532-3p/SREBF1 Axis to promote epithelial ovarian Cancer metastasis. Cancer Immunol Res. 2023;11:199–216.
33. Liang H, Geng S, Wang Y, Fang Q, Xin Y, Li Y. Tumour-derived exosome SNHG17 induced by oestrogen contributes to ovarian cancer progression via the CCL13-CCR2-M2 macrophage axis. J Cell Mol Med. 2024;28:e18315–31.
34. Tan S, Yu H, Zhang Z, Liu Y, Lou G. Hypoxic tumour-derived exosomal mir-1225-5p regulates M2 macrophage polarisation via toll-like receptor 2 to promote ovarian cancer progress. Autoimmunity. 2023;56:2281226–36.
35. Liang Y, Li J, Yuan Y, Ju H, Liao H, Li M, Liu Y, Yao Y, Yang L, Li T, Lei X. Exosomal miR-106a-5p from highly metastatic colorectal cancer cells drives liver metastasis by inducing macrophage M2 polarization in the tumor microenvironment. Volume 43. Journal of experimental & clinical cancer research: CR; 2024. pp. 281–98.
36. Xiao H, Fu J, Liu R, Yan L, Zhou Z, Yuan J. Gastric cancer cell-derived exosomal mir-541-5p induces M2 macrophage polarization through DUSP3/JAK2/STAT3 pathway. BMC Cancer. 2024;24:957–70.
37. Choi JY, Seok HJ, Lee DH, Lee E, Kim TJ, Bae S, Shin I, Bae IH. Tumor-derived mir-6794-5p enhances cancer growth by promoting M2 macrophage polarization, cell communication and signaling. Volume 22. CCS; 2024. pp. 190–208.
38. Bader JE, Wolf MM, Lupica-Tondo GL, Madden MZ, Reinfeld BI, Arner EN, Hathaway ES, Steiner KK, Needle GA, Hatem Z, Landis MD, Faneuff EE, Blackman A, Wolf EM, Cottam MA, Ye X, Bates ME, Smart K, Wang W, Pinheiro LV, Christofides A, Smith D, Boussiotis VA, Haake SM, Beckermann KE, Wellen KE, Reinhart-King CA, Serezani CH, Lee CH, Aubrey C, Chen H, Rathmell WK, Hasty AH, Rathmell JC. Obesity induces PD-1 on macrophages to suppress anti-tumour immunity. Nature. 2024;630:968–75.
39. Zhang B, Guo X, Huang L, Zhang Y, Li Z, Su D, Lin L, Zhou P, Ye H, Lu Y, Zhou Q. Tumour-associated macrophages and Schwann cells promote perineural invasion via paracrine loop in pancreatic ductal adenocarcinoma. Br J Cancer. 2024;130:542–54.
40. Li Y, Shen Z, Chai Z, Zhan Y, Zhang Y, Liu Z, Liu Y, Li Z, Lin M, Zhang Z, Liu W, Guan S, Zhang J, Qian J, Ding Y, Li G, Fang Y, Deng H. Targeting MS4A4A on tumour-associated macrophages restores CD8 + T-cell-mediated antitumour immunity. Gut. 2023;72:2307–20.
41. Ngambenjawong C, Gustafson HH, Pun SH. Progress in tumor-associated macrophage (TAM)-targeted therapeutics. Adv Drug Deliv Rev. 2017;114:206–21.
42. Lin X, Zhao R, Bin Y, Huo R, Xue G, Wu J. TIMP1 promotes thyroid cancer cell progression through macrophage phenotypic polarization via the PI3K/AKT signaling pathway. Genomics. 2024;116:110914–30.
43. Dai S, Xu F, Xu X, Huang T, Wang Y, Wang H, Xie Y, Yue L, Zhao W, Xia Y, Gu J, Qian X. miR-455/GREM1 axis promotes colorectal cancer progression and liver metastasis by affecting PI3K/AKT pathway and inducing M2 macrophage polarization. Cancer Cell Int. 2024;24:235–49.
44. Lin Y, Huang Y, Zheng Y, Chen W, Zhang Y, Yang Y, Huang W. Taurine inhibits Lung Metastasis in Triple-negative breast Cancer by modulating macrophage polarization through PTEN-PI3K/Akt/mTOR pathway. J Immunother. 2024;47:369–77.
45. Lv J, Liu C, Chen FK, Feng ZP, Jia L, Liu PJ, Yang ZX, Hou F, Deng ZY. M2-like tumour-associated macrophage-secreted IGF promotes thyroid cancer stemness and metastasis by activating the PI3K/AKT/mTOR pathway. Mol Med Rep. 2021;24:604–14.
46. Bogel G, Svab G, Muranyi J, Szokol B, Kukor Z, Kardon T, Orfi L, Tretter L, Hrabak A. The role of PI3K-Akt-mTOR axis in Warburg effect and its modification by specific protein kinase inhibitors in human and rat inflammatory macrophages. Int Immunopharmacol. 2024;141:112957–75.
47. Zhang T, Zhang Y, Yang Z, Jiang Y, Sun L, Huang D, Tian M, Shen Y, Deng J, Hou J, Ma Y. Echinococcus multilocularis protoscoleces enhance glycolysis to promote M2 macrophages through PI3K/Akt/mTOR signaling pathway, pathogens and global health, 117 (2023) 409–16.
48. Da-Wa ZX, Jun M, Chao-Zheng L, Sen-Lin Y, Chuan L, De-Chun L, Zu-Nan D, Hong-Tao Z, Shu-Qing W, Xian-Wei P, Wenbo L, Ke-Wen L. Exosomes derived from M2 macrophages exert a therapeutic effect via inhibition of the PI3K/AKT/mTOR pathway in rats with knee osteoarthritic. Biomed Res Int. 2021;2021:7218067–78.

Publisher's note